Supporting information

Optical Imaging and Spectroscopy of Atomically Precise Armchair Graphene Nanoribbons

Sihan Zhao[1], Gabriela Borin Barin[2], Ting Cao[1,3], Jan Overbeck[2], Rimah Darawish[2], Tairu Lyu[1], Steve Drapcho[1], Sheng Wang[1,4], Tim Dumslaff[5], Akimitsu Narita[5], Michel Calame[2], Klaus Müllen[5,6], Steven G. Louie[1,4], Pascal Ruffieux[2], Roman Fasel[2,7] and Feng Wang[1,4,8*]

1. Department of Physics, University of California at Berkeley, Berkeley, California 94720, United States
2. Empa, Swiss Federal Laboratories for Materials Science and Technology, 8600 Dübendorf, Switzerland
3. Department of Materials Science and Engineering, University of Washington, Seattle, WA, USA
4. Materials Science Division, Lawrence Berkeley National Laboratory, Berkeley, California 94720, United States
5. Max Planck Institute for Polymer Research, Ackermannweg 10, D-55128 Mainz, Germany
6. Johannes Gutenberg-Universität Mainz, Institute of Physical Chemistry, 5128 Mainz, Germany
7. Department of Chemistry and Biochemistry, University of Bern, Freiestrasse 3, CH-3012 Bern, Switzerland
8. Kavli Energy NanoSciences Institute at the University of California, Berkeley and the Lawrence Berkeley National Laboratory

Corresponding authors: fengwang76@berkeley.edu

<u>Figure S1.</u> An example of the optical identification of GNRs on a fused silica substrate with the correlated Raman spectroscopy.

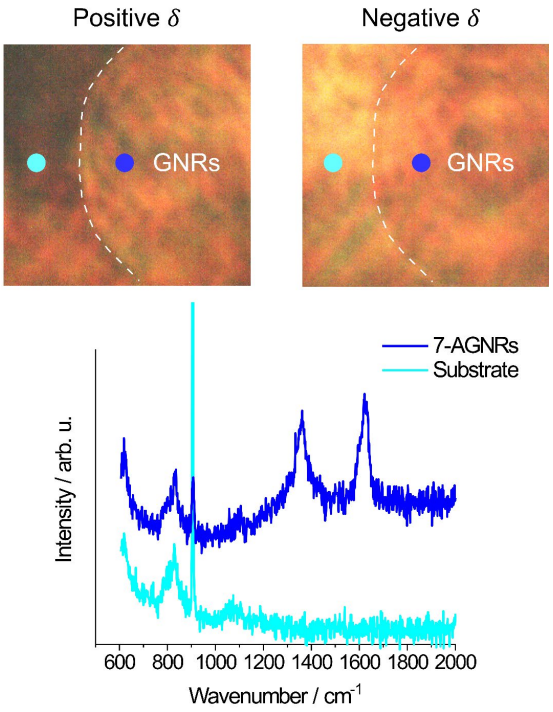

Figure S1. Microscopy imaging with the polarization spectroscopy technique and the Raman spectroscopy for 7-AGNRs. Two optical images are taken with δ at ~ 2° and at ~ -2°. The dashed lines are boundary contours separating the bare substrate on the left and GNRs on the right. GNRs appear brighter (darker) with δ at ~ 2° (~ -2°). We can observe Raman feathers of GNRs on the right of the dashed line, and that no Raman features of GNRs are detected on the left, which further confirms the successful optical identification of GNRs.

<u>Figure S2.</u> More absorption spectra of 7-AGNRs with varying polarization conditions.

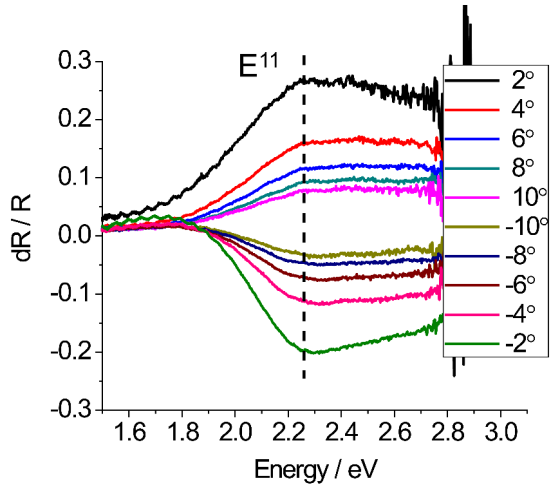

Figure S2. More data on reflection contrast spectra (dR/R) for 7-AGNRs as a function of deviation angle δ. E^{11} transition arising from the first bright exciton is indicated by dashed line.

<u>Figure S3.</u> Calculated GW bandstructure of 7-AGNR.

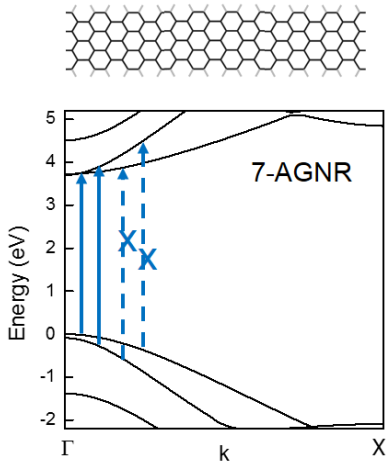

Figure S3. Calculated GW bandstructure of 7-AGNR. Solid arrows denote the first two dipole-allowed transitions E^{11} and E^{22}.

<u>Figure S4.</u> More absorption spectra of 9-AGNRs with varying polarization conditions.

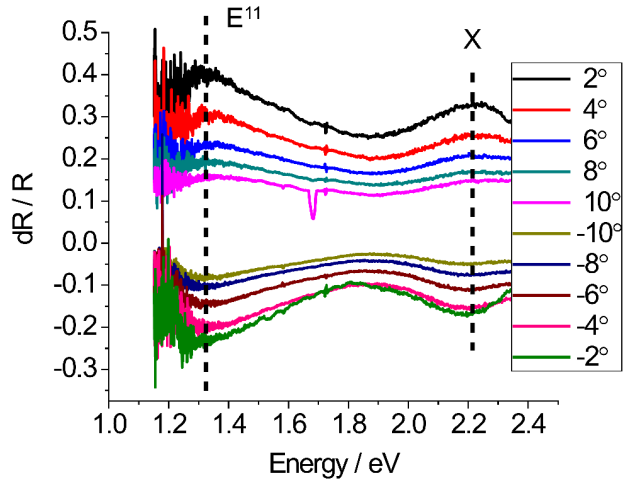

Figure S4. More data on reflection contrast spectra (dR/R) for 9-AGNRs as a function of deviation angle δ. E^{11} transition arising from the first bright exciton is indicated by dashed line. The X peak is also indicated.

<u>Figure S5.</u> Calculated GW bandstructure of 9-AGNR.

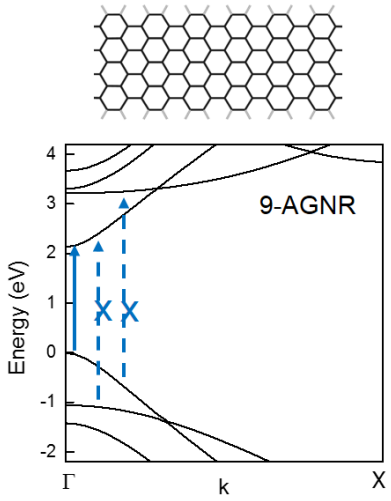

Figure S5. Calculated GW bandstructure of 9-AGNR. Solid arrow denotes the first dipole-allowed transition E^{11}.

<u>Figure S6.</u> Confirmation of E^{11} optical transition of 9-AGNRs extending to the near-IR spectral range with an InGaAs detector.

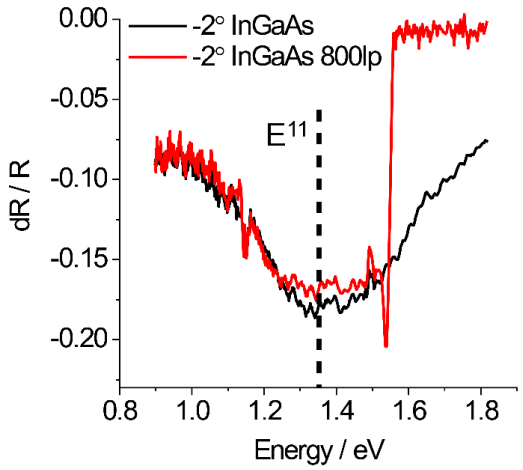

Figure S6. Reflection contrast spectra (dR/R) for 9-AGNRs with InGaAs detector taken at a deviation angle $\delta \sim$ -2°. Consistent absorption spectra with fig. 4a in the main text are obtained around the E^{11} bright exciton (indicated by dashed line). The solid red is the measurement on the same spots with 800 nm long-pass filter to exclude possible artifact from grating effect.